The Iraqi Journal For Mechanical And Material Engineering, Vol.18, No2, June 2018

EXPERIMENTAL AND NUMERICAL STUDY OF 6061-T6 AL- ALLOY FATIGUE LIFE USING FRICTION STIR WELDING

Ethar Mohamed Mahdi Mubarak
Middle Technical Univ./ Institute of Technology/Baghdad – Mech. Dept.
E-mail:etharmubark@yahoo.com

ABSTRACT
Welded parts are often subjected to variable loads. Paper's aim is to evaluate the fatigue characteristics of friction stir welding of AA6061-T6 alloy under variable loading and observed the influence of heat treatment for friction stir welding joint on the fatigue stress analysis. The microstructure of the welds alloy are studied before and after heat treatment. The friction stir welding was employed using milling machine with constant tool rotation (1000 rpm) and feed rate (20 mm/min). Artificial aging are made for aluminum friction stir welded alloy using electrical furnace at temperature of 500ºC for 20 min. Quenching at 190ºC for 4 hr. via water is followed the aging process. Fatigue test were done for specimens (base metal, friction stir welding alloys before and after heat treatment) to obtain the S-N curves for each case. Finite element via ANSYS software is used to analysis the FSW (temperature, Von-Mises stress, deformation in the welded zone and contact friction stress distributions) and Fatigue test (fatigue life, fatigue damage, fatigue safety factor, biaxiality indication , equivalent alternating stress and stress intensity factors) where the general thermo-elasto plastic relation produced under thermal and mechanical loads with isotropic, kinematic and mixed hardening rule in three dimensional problems is proposed. The results shown that the heat treatment for the friction stir welded alloy would be increased the fatigue strength of the welded plate that the number of cycles of base metal (AA6061-T6) was 1.2×10^6 and the number of cycle for welded joints without heat treatment was (0.9×10^6), where the number of cycles was 1×10^7 with heat treatment with quenching within 4hr. also it can be concluded that, the fracture opening mode (mode I) is exist in the un heated welded alloy and disappeared with heating treatment .

KEYWORDS: **Friction stir welding, 6061-T6 Al-alloys, Fatigue, ANSYS, Fatigue life, Factor of safety.**

دراسة عملية وتحليلية لعمر الكلال لسبائك الالمينيوم 6061-T6 الملحومة باللحام الاحتكاكي الدوار

ايثار محمد مهدي مبارك
الجامعة التقنية الوسطى / معهد التكنولوجيا – بغداد- قسم الميكانيك
E-mail:etharmubark@yahoo.com

الخلاصة
غالبا ما تتعرض المكونات الملحومة لاحمال متغيرة . وان الهدف من هذه الدراسة هو تقييم خصائص الكلال لسبائك الالمينيوم 6061-T6 الملحومة بالحام الاحتكاكي الدوار تحت احمال متغيرة . ودراسة خواص الكلال للقطعة الملحومة بعد معاملتها حراريا. تم دراسة التركيب المجهري للسبيكة الملحومة قبل وبعد اجراء المعاملات الحرارية حيث تم اجراء اللحام خلال ماكنة الفريزة وبسرعة دوران 1000 دورة/الدقيقة ومعدل تغذية 20ملم/دقيقة . وتمت عملية المعاملة الحرارية في فرن كهربائي ضمن درجة حرارة 500م° ولفترة 20 دقيقة ، بعدها تم التبريد في الماء يتبعها عملية التعتيق في درجة حرارة 190م° ولمدة 4 ساعات. تم اجراء فحص الكلال على العينات (السبيكة الاصلية ، السبيكة الملحومة باستخدام FSW قبل وبعد المعاملة الحرارية لايجاد منحنيات الاجهاد المتغير- عدد الدورات (S-N) لكل حالة.

Received: 2017 -10 - 10
Accepted: 2018 - 1 - 24

تم استخدام طريقة العناصر المحددة من خلال برنامج ANSYS لتحليل عملية اللحام الاحتكاكي الدوار (توزيع درجة الحرارة ، توزيع الإجهادات المكافئة، توزيع التشوهات في منطقة اللحام ، توزيع اجهادات التماس الاحتكاكية) واختبار الكلال (عمر الكلال ، الضرر ، معامل الامان ، علامة المحور الثنائي ، الاجهادات المتغيرة المكافئة و معامل شدة الاجهاد) . حيث تم اقتراح علاقة بين الانفعال والاجهاد ضمن الاحمال الحرارية والميكانيكية ولمسائل ثلاثية الابعاد في حالة كون المادة منتظمة الخواص ، حركة او حالة الخلط بينهما.
واظهرت النتائج المستحصلة ان المعاملة الحرارية للمسبوكات الملحومة بالحام الاحتكاكي الدوار ستزيد من مقاومة الكلال لهذه السبائك فتبين النتائج أن عدد دورات المعدن الأساسي (AA6061-T6) كان 1.2×10^6 وكان عدد الدورات للمفاصل الملحومة بدون المعالجة الحرارية (0.9×10^6)، حيث بلغ عدد الدورات 1×10^7 مع المعالجة الحرارية مع التبريد لمدة اربع ساعات . كما تم استنتاج أن طور الكسر الذي يحدث هو من طور(I) موجود في سبيكة ملحومة غير معاملة حراريا بينما لم يظهر اي طور للكسر عند المعاملة حراريا للملحومات .

SYMBOLS

MIG	Metal Inert Gas
TIG	Tungsten Inert Gas
GTAW	Gas tungsten arc welding
EBW	Electron beam welding
FSW	Friction stir welded
HAZ	Heat affected zone
NZ	Nugget zone
BM	Base metal
TMAZ	Thermo-Mechanically Affected Zone

INTRODUCTION

In recent years, aluminum alloys have attracted attention of many researchers, engineers and designers as promising structural materials for automotive industry or aerospace applications. (Ozturk F. et al.,2010). In results of combination welding procedures, for example, (TIG) or (MIG), hot cracking frequently happens without filler metals. These issues can be eliminated using Friction stir welding (FSW) process. FSW is another strong state joining process that offers huge advantages over customary joining forms. FSW utilizes a mix of frictional heating and compressive loading to combine metal plates that are knocked into each other and firmly clipped to the anvil of the machine (Maria Posada et al.,2003). In this way two molecularly clean metal surfaces are united under pressure and the intermetallic bond is formed. The production of heat is kept to the interface, warm information is low and the hot work connected to the weld zone brings about grain refinement. It is essential to evaluate the useful fatigue life of large welded assemblies. Fatigue is a failure mechanism that the segment fails after a timeframe in employment that it's observed the repetitive cyclic stresses (M. Ericsson and R. Sandstrom, 2003). Caizhi Zhou and Xinqi Yang (2006) explored the microstructures and properties of fatigue for friction stir welded Al– Mg alloy. FS welding had a sound joint for the absence of voids, cracks and distortions. At the point when contrasted with the base material, FSW joints displayed a better precious stone grain in the weld nugget. Y. Uematsu et al., (2008), considered the impact of microstructure and post heating treatment on fatigue conduct of the unique joints of cast aluminum composite, AC4CH-T6, and wrought aluminum compound, AA6061-T6, were contributed. Close to the weld focus, Vickers hardness is lower than in the parent metals and the hardness minima were seen along the follow course of FSW device's shoulder edge. M. K. Kulekci et al., (2008) investigated the fatigue behavior of friction stir welded butt joints of Al-1050-H8. The FSW tool rotational and transverse speeds were accepted as variable parameters. The results showed that an optimization was needed to obtain a reasonable fatigue endurance limit. Asmaa M. A. Al-Doori (2010) studied the

welding of aluminum alloy AA3003-H114 was welded by two different methods; TIG and FSW. Fatigue was tested at the optimum FSW results and compared with TIG and base metal. Many tests were examined the results of welding these tests (Tensile, Hardness, Bending, Fatigue, Micrographic, Crack propagation, and X-Ray). S. Malarvizhi and V. Balasubramanian (2011) examined the AA2219 aluminum compound square butt joints (without filler) were manufactured utilizing gas tungsten arc welding (GTAW), electron beam welding (EBW) and friction stir welded (FSW) forms. The impact of three welding forms on the fatigue crack development conduct was accounted for. Riyadh B. Mohammed (2013) investigated the influence of FSW on tensile strength, microhardness and fatigue properties of the aluminum alloy AA6061-T651. Six rotational speeds and three traverse speeds were applied, but only two tilt angles of tool, namely 0 and 2.5°. It was found that all parameters of FSW decrease both tensile strength and micro-hardness, with slight differences among parameters. The best condition was 710 rpm, 50 mm/min, and 2.5° tool tilt angle. Ahmed A. Zainalabdeen (2013) explored the fatigue conduct of friction stir welding joints for different aluminum alloys AA5052-H32 and AA7075-T6 plates of 4.82 mm thick via MTS-5-axis friction stir welding machine and scroll shoulder adjustable pin tool. Tension- tension fatigue test were done at frequently of 7 Hz.

In this work the fatigue characteristics for heated and un heated FSW welded joints are investigated experimentally and numerically via ANSYS software.

EXPERIMENTAL WORK

Material used

The base metal used in this work was 6mm thick AA6061-T6 aluminum alloy, whose chemical composition is provided in Table 1. The base metal utilized as a part of this work is 6mm thick AA6061-T6 aluminum alloy, having the chemical composition given in Table 1. The chemical composition was carried out in the Central Organization for Standardization and Quality Control / Ministry of Planning / Iraq.

Welding Process

As shown in Fig.1, the specimens with 70mm x 100mm x 6mm were longitudinal butt welded utilizing the milling machine. Every single comparable weld of 6061-T6 aluminum alloy were performed utilizing a welding device made of hardware steel. The welding device is made out of shoulder of (20mm dia.) and probe with (5mm dia. and 4.7mm length). The dimensions are suggested from the Svetsaren, ESAB, 2000, which gives the optimum mechanical properties of the welded plate as shown in Fig.2. The welding device is turned at fast and dove into the joint line between two plates to be butt welded together. In this examination, the welding parameters, for example, tool rotation (1000 rpm) and feed rate of (20mm/min) are constants.

Heat Treatment

The heat treatment precipitation incorporates arrangement heat treatment and artificial aging are made of aluminum welding joints in electric furnace with temperature of 500ºC for 20min. Quenching in water was trailed with aging process at 190ºC for 4 hr.

Microstructure Examination

The specimens produced using a cross segment of the FSW joints heated and un heated treatment compounds are ground, cleaned and carved and saw under optical magnifying lens in successions steps. Wet crushing operation with water is finished by utilizing emery paper of SiC with the distinctive grits of (220,320,500, and 1000). Cleaning process is done to the specimens utilizing diamond paste with size (1μm) with exceptional cleaning material and

grease. Then cleaned with water and alcohol and dried with warm air. Etching process is done to the specimens utilizing etching solution that is made out of (99% H2O+1%HF). At that point the specimens are washed with water and alcohol and dried.

Fatigue Test

At the point when the material is much of the time subject to changing load conditions at that point fatigue disappointment is a basic issue, that can be spoken to graphically on a S/N curve where "S" is a stress and "N" the number of cycles to failure. The specimen is performed according to the machine standard with (100 mm length) and (10mm width) as shown in Fig.3; two samples were taken for each welded plate to implement the tests.

FEM FOR THERMO-ELASTO-PLASTIC MODEL USED IN FSW

In this work, thermo-elasto-plastic model was used to simulate the FSW Process within the stir zone. In this paper the general stress -strain relation produced under thermal and mechanical loads with isotropic, kinematic and mixed hardening rule in three dimensional problems is proposed. Starting from the assumption that the total strain is separable into a (ASTM E747 ,2008):

$$d\underline{\varepsilon} = d\underline{\varepsilon}^{(e)} + d\underline{\varepsilon}^{(dm)} + d\underline{\varepsilon}^{(T)} + d\underline{\varepsilon}^{(p)} \quad (1)$$

now, from Hooke's law (ASTM E747 ,2008), $d\underline{\sigma} = [D]\,d\underline{\varepsilon}^{(e)}$,where [D] is the elasticity matrix (S.P. Timoshenko & J.N.Goodier,1970) $d\underline{\varepsilon}^{(T)} = \underline{\alpha}.dT$, the flow rule is $d\underline{\varepsilon}^{(p)} = d\lambda\,.\underline{a}$, where $\underline{a} = \partial F / \partial \underline{\sigma}$, and it can be proved that $d\underline{\varepsilon}^{(dm)} = (\partial[D]^{-1}/\partial T)\,\underline{\sigma}\,\mathrm{dT}$. Substitute all these relations into Eq.(l), it can be deduced that:

$$d\underline{\sigma} = [D]d\underline{\varepsilon} - [D](\underline{\alpha}dT + \frac{\partial[D]^{-1}}{\partial T}\underline{\sigma}dT) - [D]d\lambda\underline{a} \quad (2)$$

(i) Isotropic Hardening Rule

For isotropic hardening rule, the yield surface is function of

$$F = F(\underline{\sigma}, \underline{K}, T) \quad (3)$$

A similar postulation but without the thermal effect was proposed by Zienkiewicz et al.,1969. Differentiating F in Eq.(3) by the chain rule, it can be get (Hani Aziz Ameen,1998):

$$dF = \left(\frac{\partial F}{\partial \underline{\sigma}}\right)^t \mathrm{d}\underline{\sigma} + \frac{\partial F}{\partial k}\left(\frac{\partial k}{\partial \underline{\varepsilon}^{(p)}}\right)^t d\underline{\varepsilon}^{(p)} + \frac{\partial F}{\partial T}dT = 0 \quad (4)$$

where $K = f(k, \underline{\varepsilon}^{(p)})$. By substituting Eq.(2) into Eq.(4), and rearranged to get:

$$d\lambda = \frac{1}{\mu^{(i)}}\left(\underline{a}^t[D](d\underline{\varepsilon} - \underline{\alpha}dT - \frac{\partial[D]^{-1}}{\partial T}\underline{\sigma}dT) + \frac{\partial F}{\partial T}dT\right) \quad (5)$$

Where $\mu(i) = \underline{a}^t[D]\underline{a} - \frac{\partial F}{\partial k}\left(\frac{\partial k}{\partial \underline{\varepsilon}^{(p)}}\right)\underline{a}$. Substitute Eq.(5) into Eq.(2), it can be get

$$d\underline{\sigma}^{(i)} = [Dep]^{(i)}\,d\underline{\varepsilon} - [Dep]^{(i)}(\underline{\alpha}dT + \frac{\partial[D]^{-1}}{\partial T}\underline{\sigma}dT) - \frac{[D]\underline{a}}{\mu^{(i)}}\frac{\partial F}{\partial T}dT \quad (6)$$

Where $[Dep]^{(i)} = [D] - [D^{(p)}]^{(i)}$;and (7)

$[D^{(p)}]^{(i)} = \frac{1}{\mu^{(i)}}[D]\underline{a}\underline{a}^t[D]$. It can be found that Eq.(6) is identical to what was given in Yamada et al., 1968, without the thermal effects. To analyze the constitutive equation (Eq.(6)) with the Von Mises criterion, firstly the gradient vector $\underline{a}$ must be found as follows: the yield

surface for Von Mises is $F = \sqrt{3J_2} - \sigma_y$

where J_2 can be evaluated as (Timoshenko&J.N.Goodier ,1970)

$J_2 = \frac{1}{6}[(\sigma_1 - \sigma_2)^2 + (\sigma_2 - \sigma_3)^2 + (\sigma_3 - \sigma_1)^2]$, thus

$$\underline{a} = \frac{\partial F}{\partial \underline{\sigma}} = \frac{\partial F}{\partial J_2}\frac{\partial J_2}{\partial \underline{\sigma}} = \frac{1}{\bar{\sigma}}[M_a].\underline{\sigma} \quad (8)$$

where $$[M_a] = \begin{bmatrix} 1 & -0.5 & -0.5 & 0 & 0 & 0 \\ -0.5 & 1 & -0.5 & 0 & 0 & 0 \\ -0.5 & -0.5 & 1 & 0 & 0 & 0 \\ 0 & 0 & 0 & 3 & 0 & 0 \\ 0 & 0 & 0 & 0 & 3 & 0 \\ 0 & 0 & 0 & 0 & 0 & 3 \end{bmatrix}$$

and, the value of $\underline{a}^t[D]\underline{a} = 3G$ (9)

now, to find $\frac{\partial F}{\partial k}\left(\frac{\partial k}{\partial \underline{\varepsilon}^{(p)}}\right)^t$

we have $F = \sqrt{3J_2} - \bar{\sigma}$, thus $\frac{\partial F}{\partial k} = -\frac{\partial \bar{\sigma}}{\partial k}$ (10)

and the work done = $dk = \bar{\sigma}.d\bar{\varepsilon}^{(p)}$, hence $\frac{d\bar{\varepsilon}_{(p)}}{dk} = \frac{1}{\bar{\sigma}}$ (11)

therefore , $\frac{\partial \bar{\sigma}}{\partial k} = \frac{\partial \bar{\sigma}}{\partial \bar{\varepsilon}^{(p)}}\frac{\partial \bar{\varepsilon}^{(p)}}{\partial k} = H'\frac{1}{\bar{\sigma}}$, where $H' = \frac{d\bar{\sigma}}{d\bar{\varepsilon}^{(p)}}$

now the value of $\mu^{(i)} = 3G + \frac{H'}{\bar{\sigma}}\underline{\sigma}^t\frac{[M_a]}{\bar{\sigma}}\underline{\sigma}$

it can be proved that $\underline{\sigma}^t[M_a]\underline{\sigma} = \bar{\sigma}^2$, thus $\mu^{(i)} = 3G + H'$

After finding the value of $\mu^{(i)}$ the value of $[D^{(p)}]^{(i)}$ is

$$[D^{(p)}]^{(i)} = \frac{3G}{\bar{\sigma}^2(1+(H'/3G))}\underline{S}\underline{S}^t \quad (12)$$

Where $\underline{S} = \{S_x \quad S_y \quad S_z \quad \tau_{xy} \quad \tau_{yz} \quad \tau_{xz}\}$, $S_x = \sigma_x - \sigma_m$, $S_y = \sigma_y - \sigma_m$, and $S_z = \sigma_z - \sigma_m$

Hence, $[D_{ep}]^{(i)} = [D] - [D^{(p)}]^{(i)}$. Now, Eq.(6) will be

$$d\underline{\sigma}^{(i)} = d\underline{\sigma}^{(M)} + d\underline{\sigma}^{(T)} + d\underline{\sigma}^{(dm)} + d\underline{\sigma}^{(F)} \quad (13)$$

where: $d\underline{\sigma}^{(M)} = [D_{ep}]^{(i)}d\underline{\varepsilon}$, $d\underline{\sigma}^{(T)} = -[D_{ep}]^{(i)}\underline{\alpha}\,dT$, $d\underline{\sigma}^{(dm)} = -[D_{ep}]^{(i)}\frac{\partial[D]^{-1}}{\partial T}\underline{\sigma}\,dT$

$$d\underline{\sigma}^{(F)} = -\frac{[D]\underline{a}}{\mu^{(i)}}\frac{\partial F}{\partial T}dT$$

(ii) Kinematic Hardening Rule

For kinematic hardening rule the yield surface is (Hani Aziz Ameen,1998: $F = F(\underline{\sigma}, \underline{\hat{\alpha}}, T)$

The total differentiation of F is

$$dF = \left(\frac{\partial F}{\partial \underline{\sigma}}\right)^t d\underline{\sigma} + \left(\frac{\partial F}{\partial \alpha}\right)^t d\underline{\hat{\alpha}} + \frac{\partial F}{\partial T}dT = 0 \quad (14)$$

and it can be proved that $\frac{\partial F}{\partial \underline{\sigma}} = \frac{\partial F}{\partial \underline{\sigma}_r} = -\frac{\partial F}{\partial \underline{\hat{\alpha}}}$, where $\underline{\sigma}_r = \underline{\sigma} - \underline{\hat{\alpha}}$

from Prager shift (K. Axelsson and A. Samnelsson ,1979), $d\underline{\hat{\alpha}} = C d\underline{\varepsilon}^{(p)} = C\, d\lambda\, \underline{a}$, where $C = H'(\sigma, \varepsilon)$, thus Eq(14) will be : $dF = \underline{a}^t (d\underline{\sigma} - C\, \mathrm{d}\lambda\, \underline{\mathrm{a}}) + \frac{\partial F}{\partial T} dT$ (15)

From Eq(15) and Eq(2), it can be deduced that

$$d\lambda = \frac{1}{\mu^{(i)}} \left(\underline{a}^t\, [\mathrm{D}](\mathrm{d}\underline{\varepsilon} - \underline{\alpha} dT - \frac{\partial [D]^{-1}}{\partial T} \underline{\sigma} dT) + \frac{\partial F}{\partial T} dT \right) \quad (16)$$

Where $\mu^{(k)} = \underline{a}^t ([D]\underline{a} + C\underline{a})$. Substitute Eq(16) into Eq(2), gives

$$d\underline{\sigma}^{(k)} = [D_{ep}]^{(k)} d\underline{\varepsilon} - [D_{ep}]^{(k)} (\underline{\alpha} dT + \frac{\partial [D]^{-1}}{\partial T} \underline{\sigma}^{(k)} dT) - \frac{[D]}{\mu^{(k)}} \underline{a} \frac{\partial F}{\partial T} dT \quad (17)$$

Where $[D_{ep}]^{(k)} = [D] - [D^{(p)}]^{(k)}$; (18)

$[D^{(p)}]^{(k)} = \frac{1}{\mu} ([D]\underline{a}^{(k)} \underline{a}^{t(k)} [D])$; and $\underline{\sigma}^{(k)} = \underline{\sigma} - \underline{\hat{\alpha}}$

To analyze Eq.(17), firstly find $\underline{a}^{(k)}$, similar as in Eq.(8), hence, $\underline{a}^{(k)} = \frac{1}{\bar{\sigma}^{(k)}} [M_a] \underline{\sigma}^{(k)}$

Where $\bar{\sigma}^{(k)}$ is the effective stress of $\underline{\sigma}^{(k)}$ and the terms $((\underline{a}^t . \underline{a})^{(k)}$ will be

$$(\underline{a}^t . \underline{a}) = \frac{3}{2} \left[1 + \frac{3((\tau_{xy}{}^2 + \tau_{yz}{}^2 + \tau_{zx}{}^2)}{\bar{\sigma}^2} \right]^{(k)}$$, Hence $\mu^{(k)} = 3G + \frac{3C}{2} \left[1 + \frac{3((\tau_{xy}{}^2 + \tau_{yz}{}^2 + \tau_{zx}{}^2)}{\bar{\sigma}^2} \right]^{(k)}$

After finding the value of $\mu^{(k)}$ the value of $[D^{(p)}]^{(k)}$ is , $[D^{(p)}]^{(k)} = \frac{1}{\mu^{(k)}} \left(\frac{3G}{\bar{\sigma}^{(k)}} \right)^2 (\underline{S}\underline{S}^t)^{(k)}$

Hence, $[D_{ep}]^{(k)} = [D] - [D^{(p)}]^{(k)}$, Eq.(17) will be

$$d\underline{\sigma}^{(k)} = d\underline{\sigma}^{(M)} + d\underline{\sigma}^{(T)} + d\underline{\sigma}^{(dm)} + d\underline{\sigma}^{(F)} \quad (19)$$

where: $d\underline{\sigma}^{(M)} = [D_{ep}]^{(k)} d\underline{\varepsilon}$, $d\underline{\sigma}^{(T)} = -[D_{ep}]^{(k)}\, \underline{\alpha}\, dT$, $d\underline{\sigma}^{(dm)} = -[D_{ep}]^{(k)} \frac{\partial [D]^{-1}}{\partial T} \underline{\sigma}^{(k)}\, dT$

$$d\underline{\sigma}^{(F)} = -\frac{[D]\underline{a}^{(k)}}{\mu^{(k)}} \frac{\partial F}{\partial T} dT$$

(iii) Mixed Hardening Rule

The yield surface for mixed hardening rule is $F = F(\underline{\sigma}, \underline{\hat{\alpha}}, \underline{\varepsilon}^{(p)}, T)$ and the loading criterion may be written $f = F(\underline{\sigma}, \underline{\hat{\alpha}}, T) h^{(i)} (\underline{\varepsilon}^{(p)})$ (20)

Where $h^{(i)}$ is a function which governs the isotropic expansion or contraction of the yield surface. Hence the rate of plastic strain is now simply split into two components as (Y.Yamada, 1968, K. Axelsson,1979, Hani Aziz Ameen,1994)

$$d\underline{\varepsilon}^{(p)} = d\underline{\varepsilon}^{(p)(k)} + d\underline{\varepsilon}^{(p)(i)} \quad (21)$$

Where $d\underline{\varepsilon}^{(p)(k)} = M d\underline{\varepsilon}^{(p)}$ (22)

And $d\underline{\varepsilon}^{(p)(i)} = (1 - M) d\underline{\varepsilon}^{(p)}$ (23)

Where M<1 , Now, the total differentiation of Eq.(20), gives

$$df = \left(\frac{\partial F}{\partial \underline{\sigma}} \right)^t d\underline{\sigma} + \left(\frac{\partial F}{\partial \underline{\hat{\alpha}}} \right)^t d\underline{\hat{\alpha}} + \frac{\partial F}{\partial T} dT - \frac{dh^{(i)}}{d\varepsilon^{(p)}} d\bar{\varepsilon}^{(p)} = 0 \quad (24)$$

Having $d\underline{\hat{\alpha}} = C(1-M)d\underline{\varepsilon}^{(p)} = C(1-M)d\lambda\underline{a}^{i(k)}$, hence Eq.(24) will be

$$df = \underline{a}^{t(k)}d\underline{\sigma} - C(1-M)\underline{a}^{t(k)}d\lambda\underline{a}^{(k)} - \frac{dh^{(i)}}{d\bar{\varepsilon}^{(p)}}d\bar{\varepsilon}^{(p)} + \frac{\partial F}{\partial T}dT = 0 \qquad (25)$$

Substitute Eq.(2) into Eq.(25), it can be get :

$$d\lambda = \frac{1}{\mu^{(m)}}\left(\underline{a}^{t(k)}[D](d\underline{\varepsilon} - \underline{\alpha}dT - \frac{\partial[D]^{-1}}{\partial T}\sigma^{(k)}dT) + \frac{\partial F}{\partial T}dT - \frac{dh^{(i)}}{d\bar{\varepsilon}^{(p)}}d\bar{\varepsilon}^{(p)}\right) \qquad (26)$$

Where $\mu^{(m)} = \underline{a}^{t(k)}[D]\underline{a}^{(k)} + C(1-M)\underline{a}^{t(k)}\underline{a}^{(k)})$

Substitute Eq.(26) into Eq.(2) it can be get

$$d\underline{\sigma}^{(m)} = [D_{ep}]^{(m)}d\underline{\varepsilon} - [D_{ep}]^{(m)}(\underline{\alpha}dT + \frac{\partial[D]^{-1}}{\partial T}\underline{\sigma}^{(k)}dT) - \frac{[D]}{\mu^{(k)}}\underline{a}\frac{\partial F}{\partial T}dT + \frac{[D]\underline{a}^{(k)}}{\mu^{(m)}}\frac{dh^{(i)}}{d\bar{\varepsilon}^{(p)}}d\bar{\varepsilon}^{(p)} \qquad (27)$$

Where $[D_{ep}]^{(m)} = [D] - [D^{(p)}]^{(m)}$; and (28)

$[D^{(p)}]^{(m)} = \frac{1}{\mu^{(m)}}([D]\underline{a}^{(k)}\underline{a}^{t(k)}[D])$; and

It can be found that Eq.(27) is identical to what was found in Axelsson,1979 and Hani Aziz Ameen,1994 without the thermal effects. Hence, to analyze Eq. (27), with , $d\underline{\varepsilon}^{(p)} = d\lambda\underline{a}^{(k)}$,

$d\underline{\varepsilon}^{(p)} = \left(\frac{2}{3}(d\underline{\varepsilon}^{(p)})^{t}.d\underline{\varepsilon}^{(p)}\right)^{0.5}$ and $d\underline{\varepsilon}^{(p)(i)} = M.d\underline{\varepsilon}^{(p)}$, Eq.(26) will be

$$d\lambda = \frac{a^{t(k)}[D](d\underline{\varepsilon} - \underline{\alpha}dT - \frac{\partial[D]^{-1}}{\partial T}\sigma(k)dT + \frac{\partial F}{\partial T}dT}{a^{t(k)}[D]a^{(k)} + C(1-M)a^{t(k)}a^{(k)}) + M\frac{dh}{d\bar{\varepsilon}^{(p)(i)}}(\frac{2}{3}a^{t(k)}a^{(k)})^{0.5}} \qquad (29)$$

if we defined the abdomen of Eq.(29) as Y instead of $\mu^{(m)}$ as in Eq.(26) ,it can be get

$$Y = a^{t(k)}[D]a^{(k)} + C(1-M)a^{t(k)}a^{(k)}) + M\frac{dh}{d\bar{\varepsilon}^{(p)(i)}}(\frac{2}{3}a^{t(k)}a^{(k)})^{0.5}$$

simplified the above equation ,it can be get

$$Y = 3G + \frac{3C(1-M)}{2}\left[1 + \frac{3((\tau_{xy}{}^2 + \tau_{yz}{}^2 + \tau_{zx}{}^2)}{\bar{\sigma}^2}\right]^{(k)} + 2\bar{\sigma}_r MH'\left[1 + \frac{3((\tau_{xy}{}^2 + \tau_{yz}{}^2 + \tau_{zx}{}^2)^{(k)}}{\bar{\sigma}^{2(k)}}\right]^{0.5}$$

Where $\frac{dh}{d\bar{\varepsilon}^{(p)(i)}} = 2\bar{\sigma}_r\frac{d\bar{\sigma}_r}{d\bar{\varepsilon}^{(p)(i)}} = 2\bar{\sigma}_r H'$ and $\sigma_r = \underline{\sigma} - \underline{\hat{\alpha}} = \underline{\sigma}^{(k)}$

Hence, $[D^{(p)}]^{(m)} = \frac{1}{Y}\left(\frac{3G}{\bar{\sigma}^{(k)}}\right)^2(\underline{S}.\underline{S}^{t})^{(k)}$, and, $[D_{ep}]^{(m)} = [D] - [D^{(p)}]^{(m)}$, it can be get

$$d\underline{\sigma}^{(m)} = d\underline{\sigma}^{(M)} + d\underline{\sigma}^{(T)} + d\underline{\sigma}^{(dm)} + d\underline{\sigma}^{(F)} \qquad (30)$$

where: $d\underline{\sigma}^{(M)} = [D_{ep}]^{(m)}d\underline{\varepsilon}$, $d\underline{\sigma}^{(T)} = -[D_{ep}]^{(m)}\underline{\alpha}\,dT$, $d\underline{\sigma}^{(dm)} = -[D_{ep}]^{(m)}\frac{\partial[D]^{-1}}{\partial T}\underline{\sigma}^{(k)}\,dT$

$$d\underline{\sigma}^{(F)} = -\frac{[D]\underline{a}^{(k)}}{Y}\frac{\partial F}{\partial T}dT$$

FSW Finite Element Model via ANSYS

In this study, an adopted coupled model was used. The first part was to evaluate the temperature and its distribution (Hani Aziz Ameen ,2011), whereas the second part was to indicate the adaptive plastic deformation and material displacement (H. Tawfiq and Hani Aziz Ameen ,2000, R. M. Richard & J. R. Blacklock ,1969, S.P. Timoshenko & J.N.Goodier ,1970). A 3D coupled field (multiphysics) model was generated using ANSYS-15 software (D.R.J. Owen and E.S.Salonen ,1975). In thermal analysis, the SOLID278 element was utilized, whereas SOLID185 was used in structural analysis and SOILD226 is the coupled thermal-structural element is utilized in the coupled system. The heat generated by the tool was simulated at the penetration zone; this indicates both pin plunge and ΔT effect on the plastic deformation and material displacement at the plate edge. Stirring was modeled, in order to participate these effects on plastic deformation and material displacement. Firstly, the temperature values obtained by ANSYS. In this study, it is assumed that the tool is not rigidly solid and the work-piece is a ductile material composed of multi-linear, kinetic hardening elasto-plastic (ANSYS 15 help ,2015). Also, stress - strain curves of AA6061-T6 for different temperatures were used (ANSYS 15 help,2015). To improve modeling accuracy, a fine mesh was applied at the tool/work-piece interface. The boundary conditions (BC) at the top and bottom of the work-pieces (conduction and convection) affect the results; hence, this study adopted the BC applied by Mun and Seo (H. S. Mun and S. I. Seo ,2013). Heat generation changes according to the contact area (tool/workpiece), which produced different forces until a specific length of the shoulder (0.2 mm) dipped inside the work-piece for a period of time (ΔT). (R. Nandan ,2006, D. Jacquin ,2011).

The thermomechanical model follows the yield criteria developed by von Mises represented by Eqs.(13),(19) and (30). Their model confirmed the occurrence of transient behavior and the relationship between the stresses σ_{ij} and the strain ε_{ij} in the present study, and the variation in the physical material properties of the AA6061-T6 alloys was adopted from the study of Nandan et al.,2006 with respect to temperature, specific heat (C_p), and thermal conductivity (k).

RESULTS AND DISCUSSION

Microstructure of AA 6061-T6 welded joints without heat treatment

The microstructure results of aluminum alloy (6061-T6) that are welded by friction stir welding (FSW) process are different from parent material microstructure. Heat generated during weld this heat is change the distributed of grain and refining grain and show new phases precipitation in grain boundary. Figure(4) shows the microstructure of the cross section area of welded joint. The microstructure of nugget zone (NZ) consists of equi-axed grains in much smaller size compared to the large elongated grains of base metal (BM).

The welded nugget and TMAZ microstructures with various conditions of welding are appeared in Figure(4) Microstructures of mix zone comprise of fine equi-axed grains in all specimens. The grains in the material is deformed to recrystallize by shaping without strain grains. The grain measure is changed essentially relying upon the connected strain rate and forced warmth input. The experimental outcomes demonstrate that the higher the warmth flow the bigger the last grain sizes. This is valid for both conditions of annealed and work-hardened; be that as it may, in the work-hardening example, the current plastic strain advances recrystallization energy and microstructures with bigger grain estimate are seen in these specimens especially in TMAZ.

Microstructure of AA 6061-T6 welded joints with heat treatment

Heat treatment and artificial aging are made of AA 6061-T6 welding joints under electrical furnace with temperature of 500ºC within 20min. Quenching in water is trailed by aging process at 190ºC for 4 hrs. The microstructure results shown in Figure(5).

It's observed the microstructures of warmth influenced zone (HAZ) in the advancing and retreating sides, (b) and (d) indicated to TMAZ on the advancing and retreating sides, separately. As can be found in the pictures the bowed and prolonged TMAZ grains in the advancing side are much noticeable than in the retreating side. This might be ascribed to the direction of plastic flow out of advancing side to retreating side that creates a fiber-structure design ordinarily seen inside the metals.

S-N curves

Fatigue execution can be spoken to graphically on a S/N curve that "S" is the stress and "N" the number of cycles to failure. Friction stir welding have two group without and with heat treatment welded alloy, two groups have same variable for fatigue test such as load and dimensions specimens. Figure(6) shows the S-N curve for the base metal (Al 6061-T6). Figure(7) illustrates the S-N curve for the Al-6061-T6 welded joints without heat treatment. Heat treatment were made for FSW of AA 6061-T6 welding joints in electric furnace within temperature of 500ºC for 20min. Quenching in water is followed using the process aging at 190ºC for 4 hrs. After that the Fatigue test is done to get the S-N curve for this case as shown in Figure(8). For the purpose of toughness of each welded compared with the base metal (Figure6), the fatigue curve of the base metal (AA6061-T6) was plotted and the number of cycles was 1.2×10^6. And the number of cycle for welded joints without heat treatment was (0.9×10^6) (Figure7). As can be seen from this figure, in general the resistance of the fatigue is less than that of the base metal. This can be attributed to the fact that the heat obtained by the (FSW) has led to a change in the mineral properties, the microscopic structure of the weld. In addition, the high heat generated during the process of friction stir welding leads to the generation of residual stresses and plastic strain, which in turn weaken the mechanical properties of the weld, including the property of the fatigue.

Figure(8) shows the results of the fatigue test for samples welded with heat treatment with quenching within 4hr. where the number of cycles was 1×10^7. The welding area gave the strong mechanical properties in the fatigue test due to the release of residual stresses, the properties of the fatigue are higher than the base metal.

Temperature Distribution of FSW

Due to the difficulty in simulation, individual average force values were used with respect to pin penetration and ΔT. In FSW, heat is mainly generated by friction and plastic deformation, some formulae were developed to evaluate the influence of FSW parameters on the extent of heat generation within the welding/processing area. In FSW, the heat generated by the first touch of the pin increases the heat of the plate before the shoulder dips inside. Moreover, the material begins to plasticize in that area. Thus, the heat generated by the pin is very important in the initial welding stage, the shoulder increases this heat, especially during ΔT. The heat decreases when the tool is moved, and also it was reported that accelerating weld speed lowers temperature. Figure(9) demonstrated the temperature ascend because of heat generation. The greatest temperature on the workpiece happens under the tool. Warmth generated is because of the turning and moving pin. No outer warmth sources are utilized. As the temperature builds, the material relaxes and the coefficient of contact diminishes. A temperature-dependent coefficient of friction keeps the most extreme temperature from surpassing the material melting point (Riyadh B. Mohammed ,2013). The illustrated temperature ascend in the model demonstrated that heat generation via the load steps is because of friction between the device shoulder and workpiece.

Equivalent Stress Distribution of FSW

A standout amongst the most essential highlights of the proposed demonstrates is the capacity to foresee the equivalent stress distributions over the entire FSW process. Figure(10) demonstrates the von Mises stresses plots at six trademark time focuses, 5s, 10s, 15, 20s, 25s, and 30s from the begin of the procedure. Asymmetry dissemination of stresses is additionally an extraordinary element of FSW as it is watched. The maximum equivalent stress is moving with the tool and decreasing with time of the process.

Deformation in the welded zone of FSW

Also an essential highlight of the model is the capacity to evaluate a deflection distribution over the whole FSW process. Figure (11) shows the distribution of displacement at time points, 5s, 10s, 15, 20s, 25s, and 30s from the start of the process. From this figure it can be illustrated that deflection occurs due to heat load and the maximum deflection is moving with the tool and decreasing with time of the process.

Contact friction Stress distribution of FSW

As the instrument pivots at its area, the frictional stresses create and increment quickly. Figure (12) shows the increment in contact frictional stresses at time points, 5s, 10s, 15, 20s, 25s, and 30s from the start of the process. The values of contact frictional stresses are generated due to friction of tool and the welded plate and its produced with the rotation of tool. Heat generated from both grinding (friction) and plastic deformation is drawn against time as appeared in figures (13 and 14). Frictional energy scattering and plastic dispersal increment in a bilinear way have been shown. There is a smooth progress locale around 12s and generation rates end up plainly higher after 13.5s. In the present model outcomes, friction was in charge of producing a large portion of the warmth required notwithstanding when full contact condition had built up and extreme plastic distortion happened. Figure(13) watched the generation of warmth because of plastic distortion on the workpiece. The yield alternative of component SOLID226 gives the plastic warmth generation rate per unit volume. Figure(14) illustrated the heat generation because of friction and plastic distortion produced heat. A figuring of frictional and plastic warmth generation is implemented, starts with the first load step. Figure(15) illustrated the greatest temperature go at the weld line area on the workpiece under the device's tool is good beneath the liquefying temperature of the workpiece via the load steps. Plainly watched that friction is in charge of producing a large portion of the required warmth, while the commitment of warmth because of plastic distortion is less noteworthy.

Welded joints analysis (ANSYS results)

Fatigue is the failure of a material under fluctuating stresses each of which is believed to produce minute amounts of plastic strain (Mustafa Kemal Kulekci et al.,2008), failure is the sudden fracture after initiation and growth of a crack. The module is incorporated into the ANSYS Workbench Environment. From the test of fatigue, the fracture opening mode (mode I) is exist in the un heated welded alloy associated with local displacements in which the cracks surface move apart in a direction perpendicular to the surface.

Fatigue Life

ANSYS Workbench demonstrated the outcome form plot demonstrated the accessible life for the given fatigue investigation, as appeared in Figure(16).

Fatigue Damage
It is a contour plot of the fatigue damage at a given design life. Fatigue damage is defined as the design life divided by the available life, as shown in Figure(17).

Safety Factor of Fatigue
It is a shape plot of the safety factor as for the fatigue failure at a given outline life. The greatest Safety Factor showed is 15. Like damage and life, this outcome might be perused. For Fatigue Safety Factor, values short of what one demonstrate disappointment before the outline life is come to, as appeared in Figure(18).

Biaxiality indication
It is characterized as the principal stress littler in extent separated by the bigger principal stress with the main stress closest zero disregarded. A biaxiality of zero compares to uniaxial stress as appeared in Figure(19).

Equivalent Alternating Stress
It is the stress used to inquiry the SN curve of fatigue in the wake of representing fatigue loading sort, mean stress impacts, multiaxial impacts, and some other parameters in the fatigue investigation, as appeared in Figure(20).

Stress Intensity Factor
The stress components near the crack is proportional to a single constant factor (*K).* If this constant is known, the entire stress distribution at the crack tip can be computed. This constant, which is called the stress-intensity factor as shown in Figure(21).

CONCLUSIONS

1. The simulation results are presented in this paper shown that the fatigue strength of welded FSW joints is significantly improved with heat treatment welded alloy. This simulation gives the advantage to visualize damaged areas and allows to optimize the lifetime of structures; to avoid significant damage and loss of life. Due to the differences of microstructure present in FSW welds under heated treatment and un heated treatment, highly differences in mechanical behavior in each of the areas (BM, HAZ, TMAZ and Nugget is existed .
2. The microstructure of the metal has been improved and refinement after heat treatment.
3. The number of cycles of base metal (AA6061-T6) was 1.2×10^6. And the number of cycle for welded joints without heat treatment was (0.9×10^6), where the number of cycles was 1×10^7 with heat treatment with quenching within 4hr.
4. It can be concluded that mode I (fracture opening mode) is observed in the un heated welded alloy associated with local displacements in which the cracks surface move apart in a direction perpendicular to the surface.

Table 1 Chemical composition of 6061 Al T6 alloy

Element wt%	Mg	Si	Fe	Mn	Cu	Cr	Zn	Al
Measured value	1.03	0.778	0.6	0.14	0.082	0.09	0.03	Rem
Standard value [12]	0.8-1.2	0.4-0.8	Max 0.7	Max 0.15	0.15-.40	0.04-.35	Max 0.25	Rem

Fig.1 Milling Machine

Fig.2 Welding tool

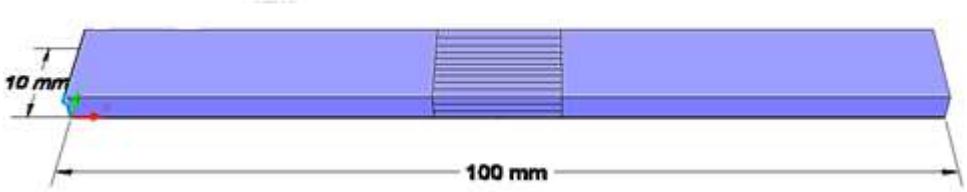

Fig.3 Sample of fatigue test

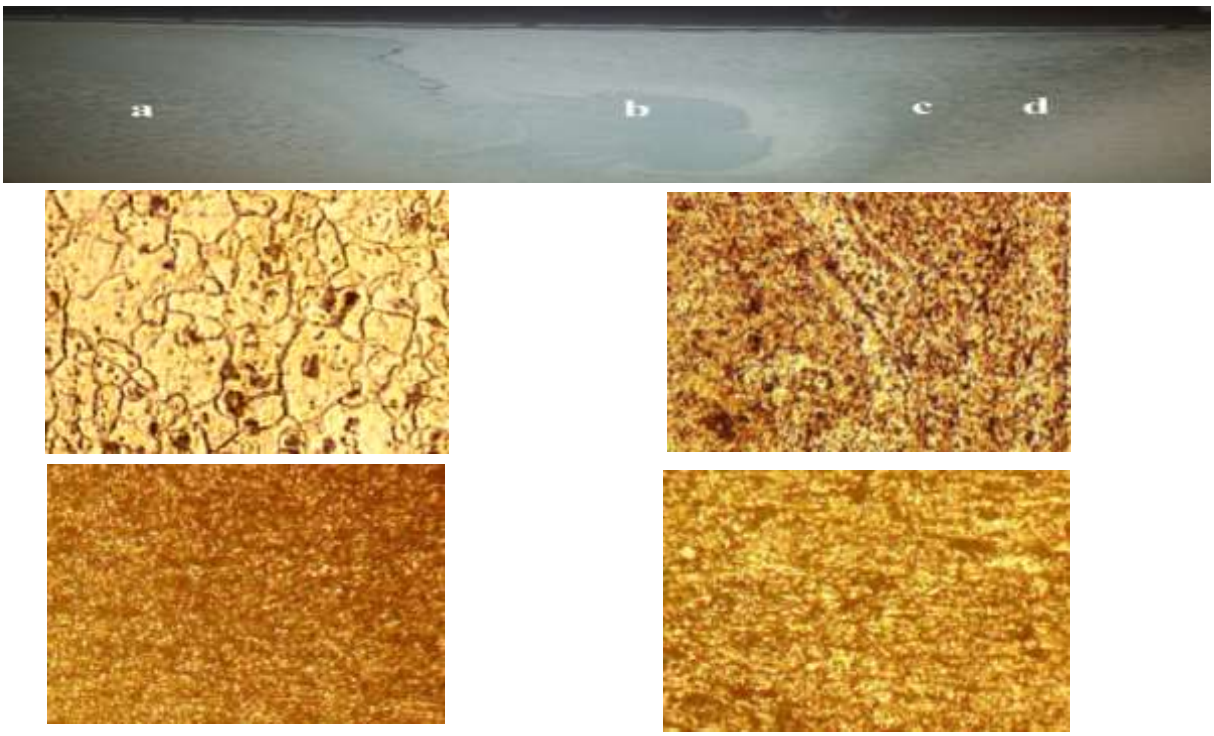

Fig.4 Microstructure of different areas in cross section of FSW joint of Al (X 50µm)
(a) HAZ (b) Nugget zone (c) TMAZ (d) TMAZ

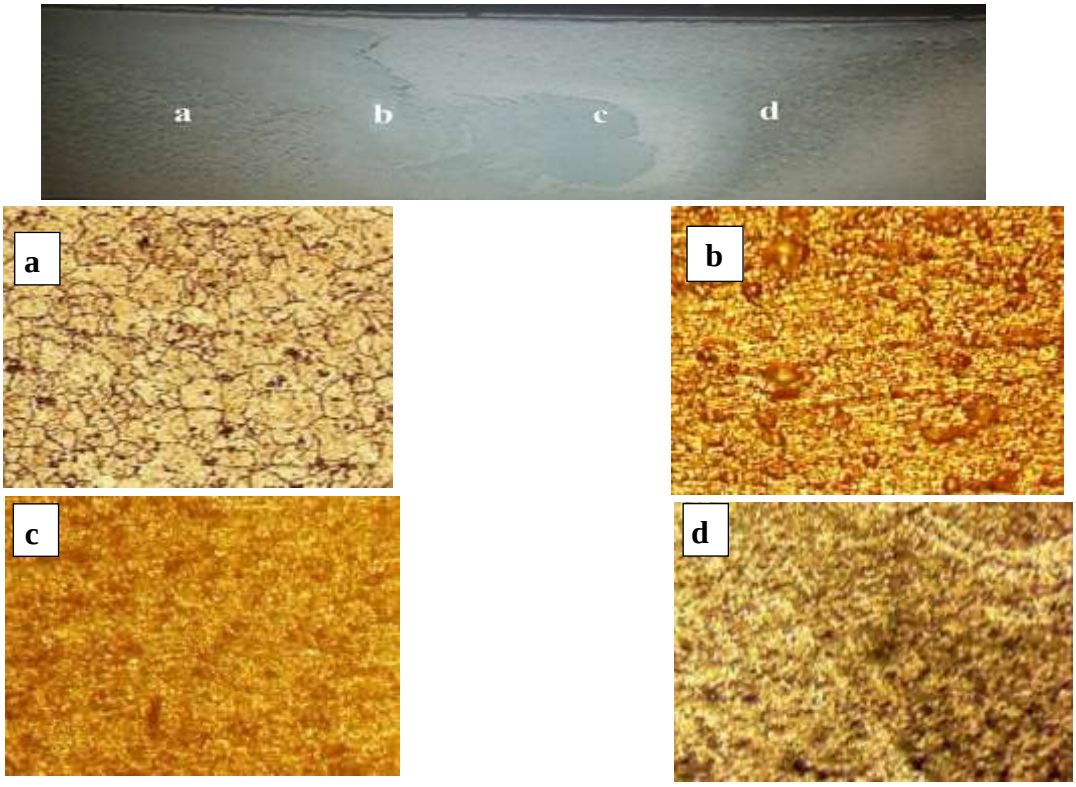

Fig.5 Microstructure of various regions in cross section of FSW joint of Al 6061-T6 after heat treatment. (X 50µm)
(a) HAZ (b) TMAZ (c) Nugget zone (d) TMAZ

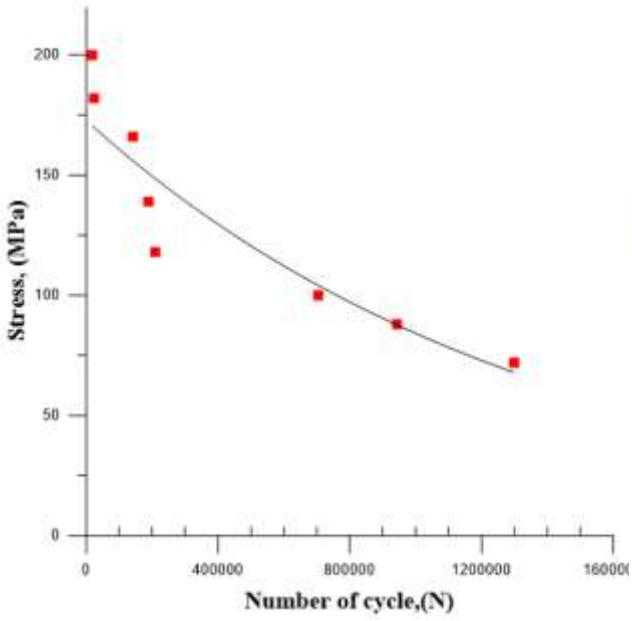

Fig.6 S-N curve of (AA6061-T6) base metal

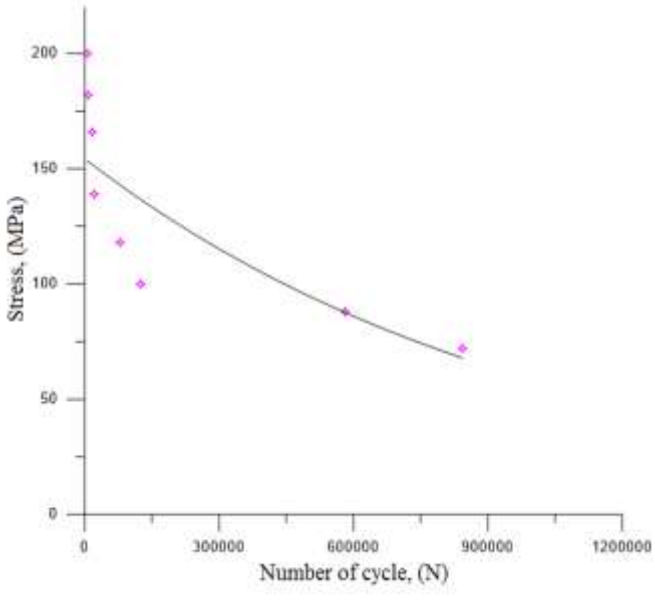

Fig.7 S-N curve of (AA6061-T6) welded joints without heat treatment

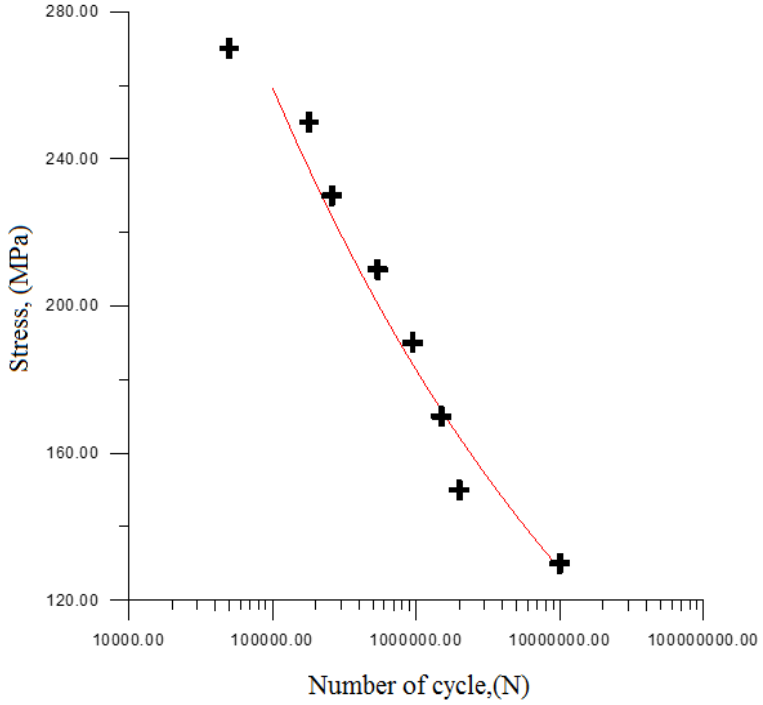

Fig.8 S-N curve of (AA6061-T6) welded joints with heat treatment

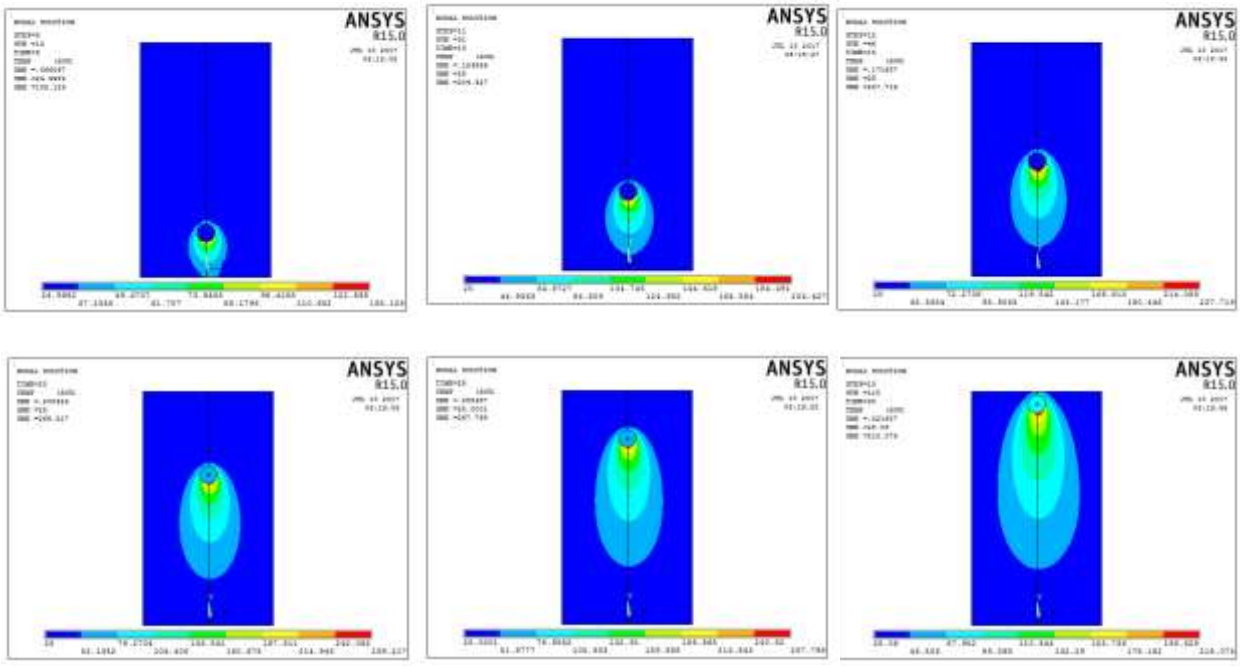

Fig.9 Temperature distribution with moving tool

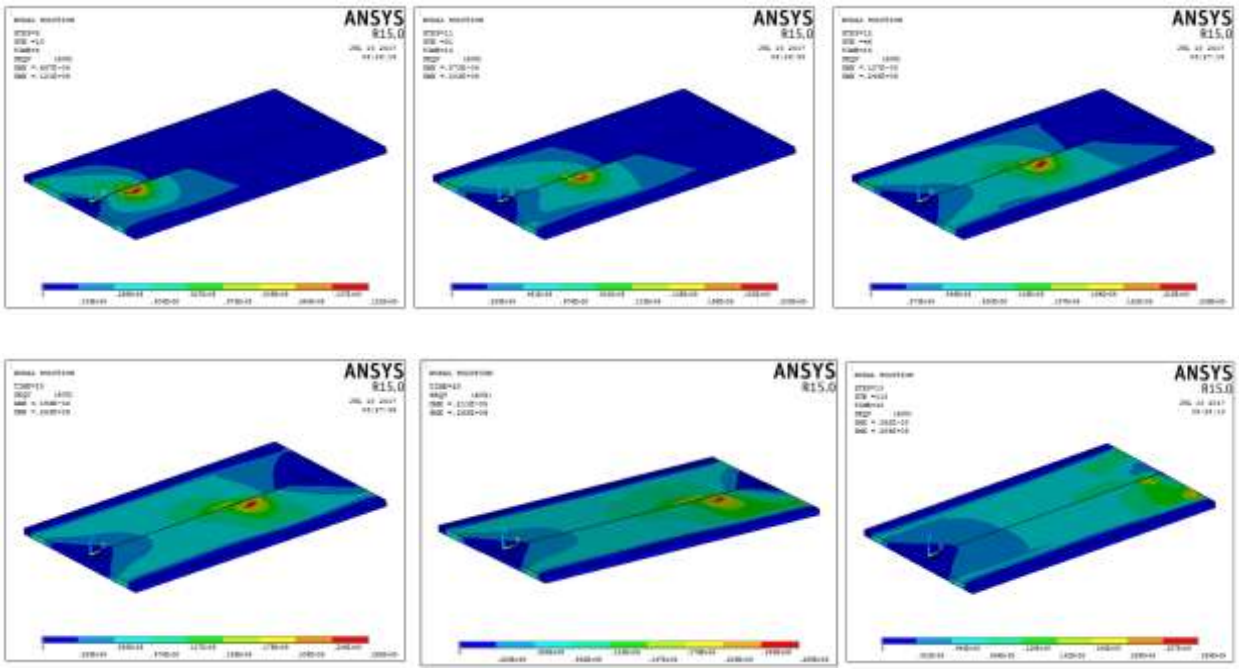

Fig.10 Equivalent stress distribution with moving tool

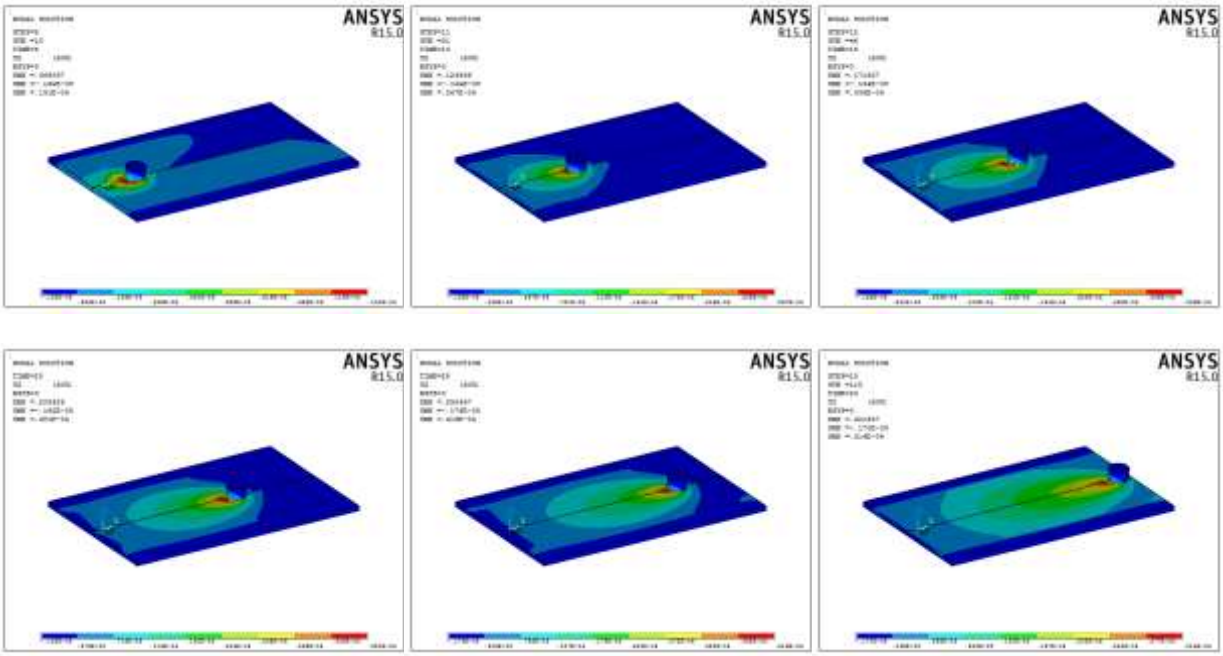

Fig.11 Deformation in the welded zone with moving tool

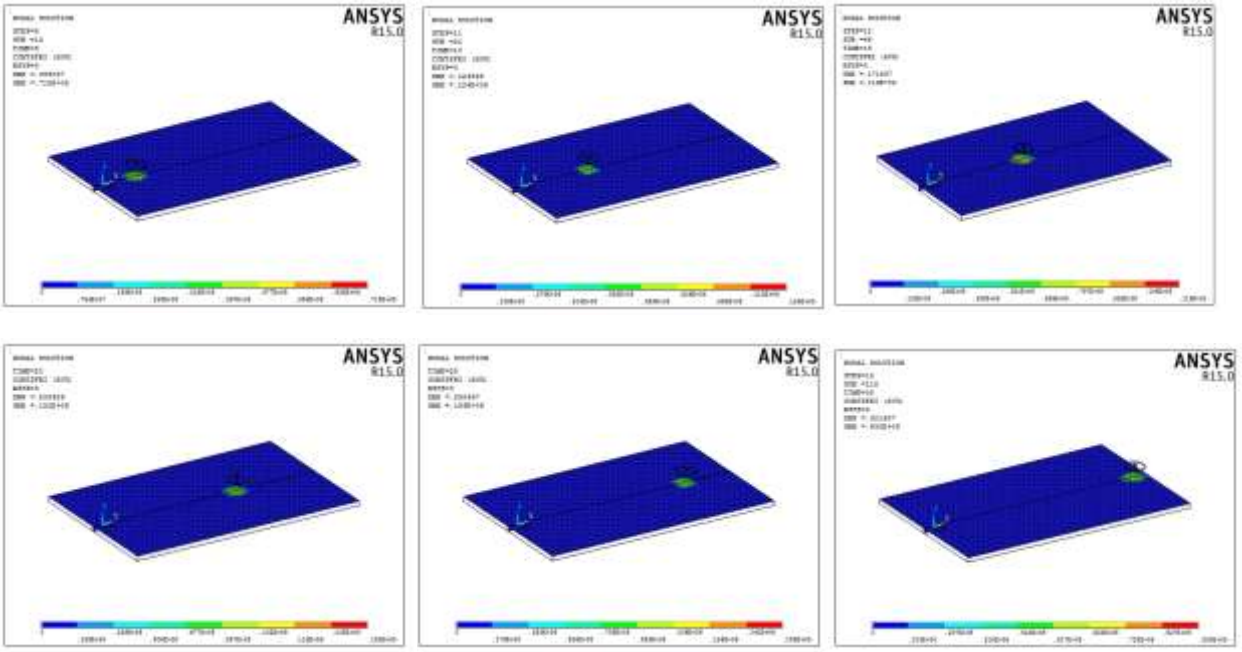

Fig.12 Contact friction stress with moving tool

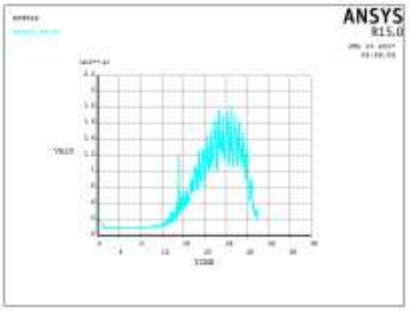

Fig.13 Plastic heat against time

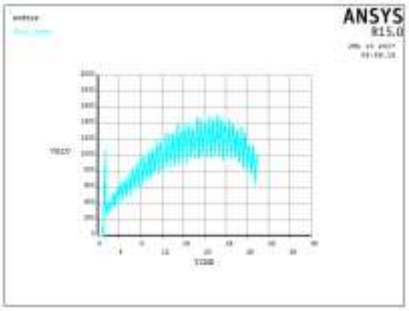

Fig.14 Friction heat against time

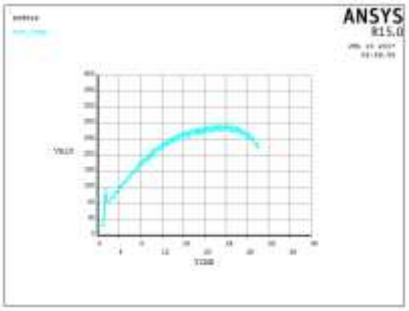

Fig.15 Max. Temp. against time

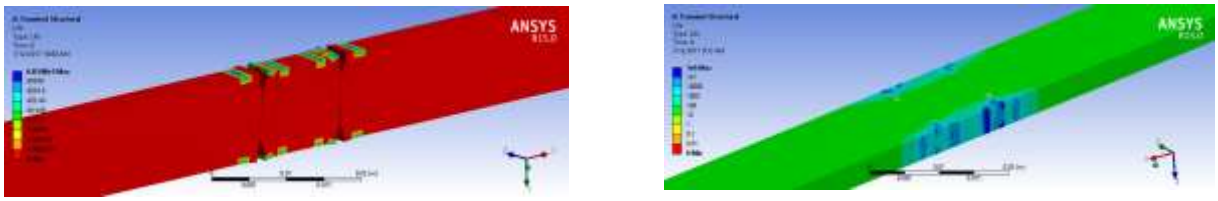

(a) **(b)**

Fig.16 **(a)** un heated FSW alloy **(b)** heated FSW alloy

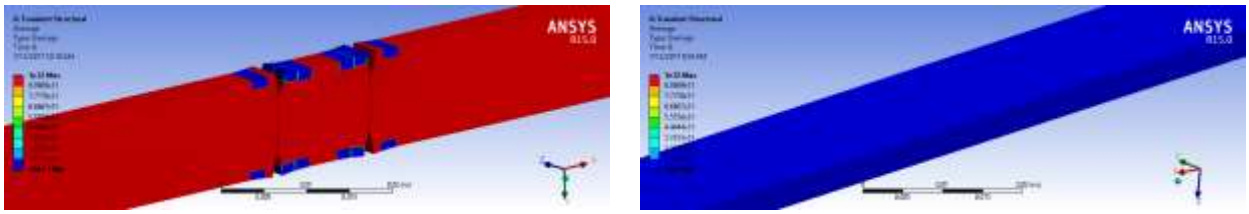

(a) **(b)**

Fig.17 (a) un heated FSW alloy **(b)** heated FSW alloy

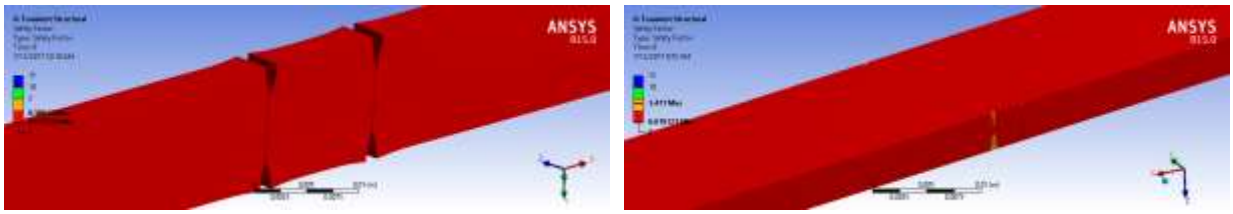

(a) **(b)**

Fig.18 (a) un heated FSW alloy **(b)** heated FSW alloy

(a) **(b)**

Fig.19 (a) un heated FSW alloy **(b)** heated FSW alloy

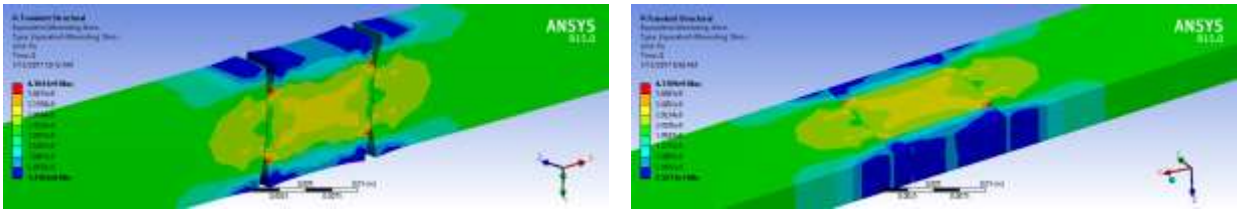

(a) **(b)**

Fig.20 (a) un heated FSW alloy **(b)** heated FSW alloy

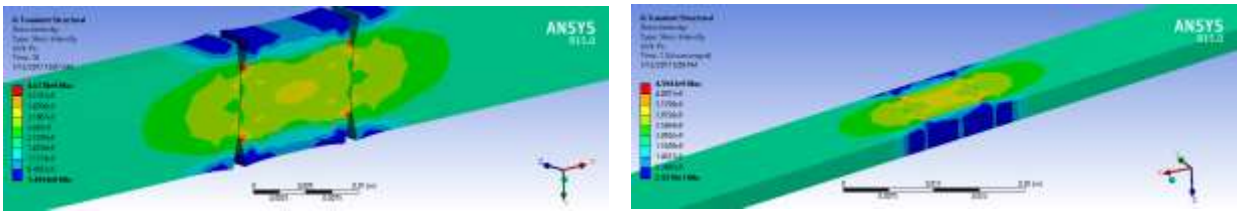

(a) **(b)**

Fig.21 (a) un heated FSW alloy **(b)** heated FSW alloy

REFERENCES

Ahmed A. Zainulabdeen “Investigation of Fatigue Properties of Dissimilar Aluminum Joints by Friction Stir Welding” Ph.D. Thesis, University of Technology/ Department of Production Engineering & Metallurgy-Iraq, (2013).

ANSYS 15 help, “ ANSYS Theory Reference”, (2015).

Asmaa M. A. Al-Doori "Fatigue Properties of Friction Stir Welded Aluminum Alloys", M.Sc. Thesis, Al-Nahrain University/ College of Engineering, Iraq, December (2010).

ASTM E747," Standard Practice for Design, Manufacture and Material Grouping Classification of Wire Image Quality Indicators (IQI) Used for Radiology،” (2008).

C. M. Chen and R. Kovacevic, “Finite element modeling of friction stir welding: thermal and thermomechanical analysis,” *International Journal of Machine Tools and Manufacture*, Vol. 43, No. 13, pp:1319–1326, (2003).

Caizhi Zhoua and Xinqi Yang,"Investigation of microstructures and fatigue properties of friction stir welded Al–Mg alloy”, Materials Chemistry and Physics , Vol.98 ,pp: 285–290, (2006).

D. Jacquin, B. deMeester, A. Simar, D. Deloison, F.Montheillet, and C. Desrayaud, “A simple Eulerian thermomechanical modeling of friction stir welding,” *Journal of Materials Processing Technology*, Vol. 211, No.1, pp:57–65, (2011).

D.R.J. Owen and E.S.Salonen "Three-dimensional elasto-plastic finite element Analysis", Int. J. for .Num. Meth. Eng., Vol.9 , pp:209-218, (1975).

H. S. Mun and S. I. Seo, “Welding strain analysis of friction stir welded aluminum alloy structures using inherent strain-based equivalent loads,” *journal of Mechanical Science and Technology*, Vol. 27, No. 9, pp:2775–2782, (2013).

H. Tawfiq and Hani Aziz Ameen “Three dimensional heat transfer finite element analysis with steady state ,transient and phase change “ . Engineering and Technology Journal, Vol.19, No.5, (2000).

Hani Aziz Ameen , “Finite Element Method for Thermo-Elasto-Plastic Stress Analysis of Three Dimensional Problems”, Ph.D. thesis, University of Technology, Mechanical Engineering Dept., Iraq, (1998).

Hani Aziz Ameen “Derivation of lagrangian shape functions for hexahedral element”. IeJAAEM , Vol 1, Jan, (2011). (http://www.ieems.org)

Hani Aziz Ameen “FEM for elasto-plastic stress analysis of two dimensional problems”. M.Sc. thesis, Al-Nahreen university, (1994).

K. Axelsson and A. Samnelsson “Finite element analysis of elastic-plastic material displaying mixed hardening", Int. J. Num. Eng., Vol.14, pp:211-225, (1979).

M. Ericsson and R. Sandstrom, "Influence of welding speed on the fatigue of friction stir welds, and comparison with MIG and TIG", International Journal of Fatigue,Vol.25, pp:1379–1387, (2003).

Maria Posada, P. Jennifer Nguyen, R. David Forrest, J. Jobnnie Branch and Robert Denale, "Friction Stir Welding Advances Joining Technology", *Special Issue AMPIAG, Quarterly* Vol. 7, No.3, pp:13-20, (2003).

Mustafa Kemal Kulekci , Aydin *Ş*ik and Erdinç Kaluç," Effects of tool rotation and pin diameter on fatigue properties of friction stir welded lap joints" Int. J. Adv. Manuf. Technol. , Vol.36, pp:877–882, (2008).

O.C. Zienkiewicz, S. Valliappan and I .P. King "elasto-plastic solutions of engineering problems 'initial stress', finite element approach", Int. J. for Num. Meth. Eng. Vol.1, pp:75-100,(1969).

Ozturk F., Sisman A., Toros S., Kilic S., and Picu R.C., "Influence of aging treatment on mechanical properties of 6061 aluminum alloy", *Materials and Design* Vol. 31, pp: 972–975, (2010).

R. M. Richard & J. R. Blacklock " Finite element analysis of inelastic structures" AIAA. J. (7) (3),pp:432-438,(1969).

R. Nandan, G. G. Roy, and T. Debroy, "Numerical simulation of three dimensional heat transfer and plastic flow during friction stir welding," *Metallurgical and Materials Transactions A: Physical Metallurgy and Materials Science*, Vol. 37, No. 4, pp:1247–1259, (2006).

Riyadh B. Mohammed," Influence of friction stir welding Parameters on static and dynamic Mechanical properties of aluminum alloy (AA 6061-T651)", M.Sc. thesis, Middle Technical University, (2013).

S. Malarvizhi and V. Balasubramanian " Fatigue crack growth resistance of gas tungsten arc, electron beam and friction stir welded joints of AA2219 aluminium alloy", Materials and Design, Vol.32 , pp:1205–1214, (2011).

S.P. Timoshenko & J.N.Goodier "Theory of elasticity ",3rd edn, McGraw-Hill, (1970).
Svetsaren, ESAB,"A welding Review ", Vol.54, No. 2, pp: 12-13, (2000).

Y. Uematsu , K. Tokaji , Y. Tozaki , T. Kurita and S. Murata, "Effect of re-filling probe hole on tensile failure and fatigue behavior of friction stir spot welded joints in Al–Mg–Si alloy" International Journal of Fatigue, Vol.30, pp:1956–1966, (2008).

Y.Yamada, N.Yoshimura & T. Sakurai "Plastic stress -strain matrix and its application for the solution of elastic plastic problem by FEM", Int. J. Mech. Sci. (10), pp:343-354,(1968).